Int J Physiol Pathophysiol Pharmacol 2016;8(1):14-27
www.ijppp.org /ISSN:1944-8171/IJPPP0026410

Original Article

The mitochondria-targeted antioxidant MitoQ attenuates liver fibrosis in mice

Hasibur Rehman[1,5*], Qinlong Liu[1,6*], Yasodha Krishnasamy[1], Zengdun Shi[2], Venkat K Ramshesh[1], Khujista Haque[1], Rick G Schnellmann[1,7], Michael P Murphy[4], John J Lemasters[1,3,8], Don C Rockey[2], Zhi Zhong[1]

[1]Departments of Drug Discovery & Biomedical Sciences, [2]Medicine, [3]Biochemistry & Molecular Biology, Medical University of South Carolina, Charleston, SC 29425, USA; [4]MRC Mitochondrial Biology Unit, Wellcome Trust/MRC Building, Cambridge CB2 0XY, U.K.; [5]Department of Biology, Faculty of Sciences, University of Tabuk, Saudi Arabia; [6]The Second Affiliated Hospital of Dalian Medical University, Dalian, Liaoning Province, China; [7]Ralph H. Johnson VA Medical Center, Charleston, SC 29403, USA; [8]Institute of Theoretical & Experimental Biophysics, Russian Academy of Sciences, Pushchino, Russian Federation. [*]Equal contributors.

Received February 22, 2016; Accepted March 15, 2016; Epub April 25, 2016; Published April 30, 2016

Abstract: Oxidative stress plays an essential role in liver fibrosis. This study investigated whether MitoQ, an orally active mitochondrial antioxidant, decreases liver fibrosis. Mice were injected with corn oil or carbon tetrachloride (CCl_4, 1:3 dilution in corn oil; 1 μl/g, ip) once every 3 days for up to 6 weeks. 4-Hydroxynonenal adducts increased markedly after CCl_4 treatment, indicating oxidative stress. MitoQ attenuated oxidative stress after CCl_4. Collagen 1α1 mRNA and hydroxyproline increased markedly after CCl_4 treatment, indicating increased collagen formation and deposition. CCl_4 caused overt pericentral fibrosis as revealed by both the sirius red staining and second harmonic generation microscopy. MitoQ blunted fibrosis after CCl_4. Profibrotic transforming growth factor-β1 (TGF-β1) mRNA and expression of smooth muscle α-actin, an indicator of hepatic stellate cell (HSC) activation, increased markedly after CCl_4 treatment. Smad 2/3, the major mediator of TGF-β fibrogenic effects, was also activated after CCl_4 treatment. MitoQ blunted HSC activation, TGF-β expression, and Smad2/3 activation after CCl_4 treatment. MitoQ also decreased necrosis, apoptosis and inflammation after CCl_4 treatment. In cultured HSCs, MitoQ decreased oxidative stress, inhibited HSC activation, TGF-β1 expression, Smad2/3 activation, and extracellular signal-regulated protein kinase activation. Taken together, these data indicate that mitochondrial reactive oxygen species play an important role in liver fibrosis and that mitochondria-targeted antioxidants are promising potential therapies for prevention and treatment of liver fibrosis.

Keywords: Antioxidant, hepatic stellate cell, liver fibrosis, mitochondria, MitoQ, oxidative stress

Introduction

Liver fibrosis/cirrhosis affects more than 100 million people worldwide and represents one of the most common causes of death in adults [1, 2]. Moreover, cirrhosis markedly increases the risk of hepatocellular carcinoma (HCC), and about 75% of HCC occurs on the basis of liver fibrosis. Despite extensive studies, the mechanisms of fibrosis are not well understood, and effective therapies are lacking [2, 3]. Liver fibrosis/cirrhosis ultimately leads to end-stage liver disease, which requires liver transplantation. However, this resource is limited [4], and many patients die while waiting for a transplant. Therefore, the ideal approach to management of patients with chronic liver disease would be to understand the mechanisms of fibrosis in order to develop mechanism-based, effective therapies to inhibit the progression of and/or reverse fibrosis/cirrhosis.

Liver fibrosis represents a wound healing response to chronic liver injury. Liver injury stimulates a multicellular response involving multiple resident hepatic cells. In particular, hepatic stellate cells (HSCs) play a key role with their activation leading to formation and deposition of collagen-rich extracellular matrix (ECM) [1, 2, 5, 6]. Multiple other cell types, including injured hepatocytes, activated Kupffer cells, stimulated cholangiocytes, and various infiltrating cells (e.g. leukocytes and platelets), appear to fuel the fibrotic process by producing cytokines,

chemokines, growth factors, miRNAs, reactive oxygen species (ROS) and/or damage-associated molecular pattern molecules (DAMPs) [1, 2, 7].

Clinical and experimental studies suggest that oxidative stress plays an important role in the development of fibrosis [8-10]. Oxidative stress is common in different types of chronic liver injury [11-13]. ROS not only induce hepatocyte damage/death but also stimulate/amplify inflammatory and profibrotic responses [8-13]. Our previous study showed that antioxidant green tea polyphenols decreased cholestatic liver fibrosis in rats [14]. Interestingly, over-expression of mitochondrial superoxide dismutase-2 (SOD2, which degrades superoxide radicals) attenuated liver injury and fibrosis much better than over-expression of cytosolic SOD1, suggesting mitochondrial oxidative stress plays a crucial role in development of liver fibrosis [15].

Mitochondria are a major source of ROS in cells [16, 17]. Mitochondrial ROS production mediates pathological processes in many diseases and in aging [18]. Therefore, in recent years increasing efforts have focused on development of mitochondria-targeted antioxidants. MitoQ ([10-(4,5-dimethoxy-2-methyl-3,6-dioxo-1,4-cyclohexadien-1-yl)decyl]triphenyl-, methanesulfonate) is a derivative of the potent antioxidant ubiquinone conjugated to triphenylphosphonium (TPP), which enables MitoQ to enter and accumulate within mitochondria [19]. As such, MitoQ is more effective in preventing mitochondrial oxidative damage compared to untargeted antioxidants. MitoQ has been found effective *in vitro*, in animals, and in humans in attenuating cell/tissue damage in many situations, including Parkinson's disease, aging, colitis, metabolic syndrome, hepatitis C, and cardiac dysfunction [20-25]. Since mitochondrial ROS may be crucial in development of liver fibrosis, we explored whether decreased mitochondrial oxidative stress by MitoQ ameliorates liver fibrosis in vivo and directly inhibits HSC activation *in vitro*.

Methods

In vivo liver fibrosis model and MitoQ treatment

Liver fibrosis was induced *in vivo* by carbon tetrachloride (CCl_4) treatment, one of the most widely used experimental liver fibrosis models [26, 27]. Male C57BL/6J mice (8-9 weeks, Jackson Laboratory, Bar Harbor, Maine) were allowed access to drinking water containing 500 μM MitoQ or the inactive comparison compound (decylTPP, both from the MRC Mitochondrial Biology Unit, Cambridge, U.K.) *ad libitum*. Three days after starting MitoQ, mice were injected with CCl_4 (Sigma, St. Louis, MO; 1:3 dilution in corn oil; 1 μl of the dilution/g, *i.p.*) or an equal volume of corn oil once every 3 days for up to 6 weeks [26, 27]. MitoQ was given throughout the CCl_4 treatment period. All animals received humane care in compliance with institutional guidelines. Animal protocols were approved by the Institutional Animal Care and Use Committee.

Alanine aminotransferase (ALT) measurement

After 5 and 6 weeks of CCl_4 treatment, mice were anesthetized with pentobarbital (80 mg/kg, *i.p.*), and blood was collected from the inferior vena cava. Serum alanine transaminase (ALT) was measured using a kit from Pointe Scientific (Canton, MI).

Histology and immunohistochemical staining

Livers were harvested under pentobarbital anesthesia after rinsing with ~2 mL normal saline. Liver tissue was fixed and processed for paraffin sections, as described elsewhere [28]. In liver sections stained with hematoxylin and eosin (H&E), histological images were captured under a microscope (Zeiss Axiovert 100 microscope, Thornwood, NY) using a 20x objective lens.

Apoptosis was detected on liver slides by terminal deoxynucleotidyl transferase-mediated dUTP nick-end labeling (TUNEL) using an *In Situ* Cell Death Detection Kit according to the manufacturer's protocol [29]. TUNEL-positive and negative cells were counted in a blinded manner in 10 randomly selected fields using a 40x objective lens.

Liver fibrosis was analyzed on liver slides by 2 different methods. Some liver slides were stained with 0.1% sirius red (Polysciences Inc., Warrington, PA) and fast green FCF (Sigma-Aldrich, St. Louis, MO) to reveal liver fibrosis, and light microscopic images were captured using a 10x objective lens [14].

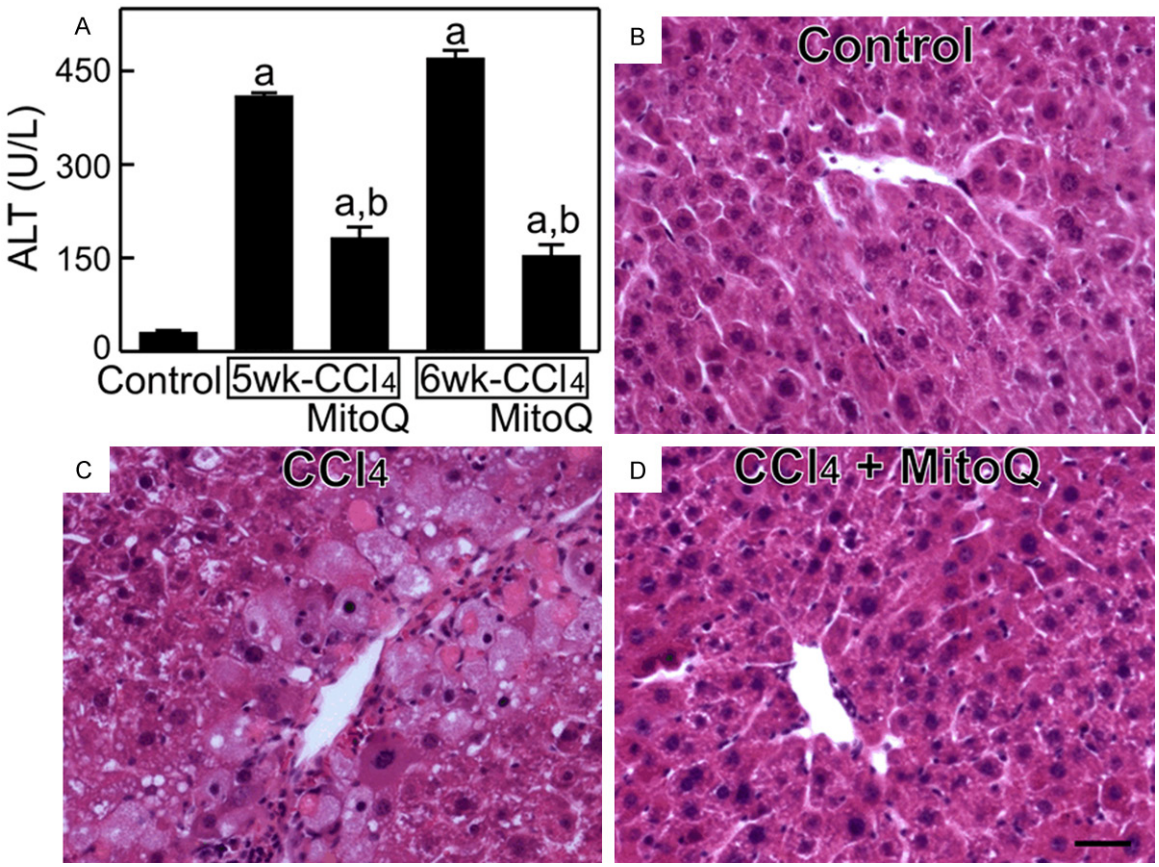

Figure 1. MitoQ attenuates liver injury after CCl_4 treatment in vivo. CCl_4 was administered to mice as in Methods, and MitoQ or decylTPP was added to the drinking water of some animals. The control group received vehicle (corn oil and decylTPP) for 6 weeks. A: Blood was collected at 5 and 6 weeks of CCl_4 treatment and alanine aminotransferase (ALT) was measured. Values are means ± SEM. a, $p<0.05$ vs control; b, $p<0.05$ vs the corresponding CCl_4 group. B-D: Representative images of H&E slides after 6 weeks of CCl_4 treatment (n = 4/group).

Liver fibrosis was also revealed by second harmonic generation (SHG) microscopy of liver sections. When intense laser light passes through a material with a non-linear, noncentrosymmetric molecular structure (e.g., collagen and muscle myosin), 2 photons with the same frequency in the laser light can interact with the nonlinear material to generate a new photon possessing twice the energy and hence half the wavelength of the original photons [30]. Imaging of the SHG emission allows visualization of collagen fibers without the use of stains or fluorophores, which avoids non-specific staining that occurs frequently in injured tissue using other methods. SHG imaging was performed on de-paraffinized, unstained slides using a Zeiss LSM 510 NLO laser scanning confocal/multiphoton microscope (Thornwood, NY) and a 25x 0.8 NA water-immersion objective lens. Two-photon excitation was performed with 900-nm light from a Coherent Chameleon Ultra laser. The emission wavelength was 450 nm.

Measurement of hydroxyproline in liver tissue

About 100 mg of frozen liver tissue was hydrolyzed in 1 ml of 2 N NaOH at 120°C in a heating block for 20 minutes. The hydrolysates were centrifuged at 10,000 rpm for 10 min at room temperature. The supernatant was mixed gently with 450 µl chloramine-T reagent (Sigma-Aldrich, St. Louis, MO) and kept at room temperature for 25 minutes. Finally, 500 µl of Ehrlich's aldehyde reagent (Mallinckrodl Baker Inc., Phillipsburg, NJ) containing 5% (w/v) p-dimethylaminobenzaldehyde in *n*-propanol/perchloric acid (2:1, v/v) was added to each sample, and the chromophore was developed by incubating the samples at 65°C for 20 minutes. Absorbance was measured at 550 nm using a SpectraMax M2 spectrophotometer/micropla-

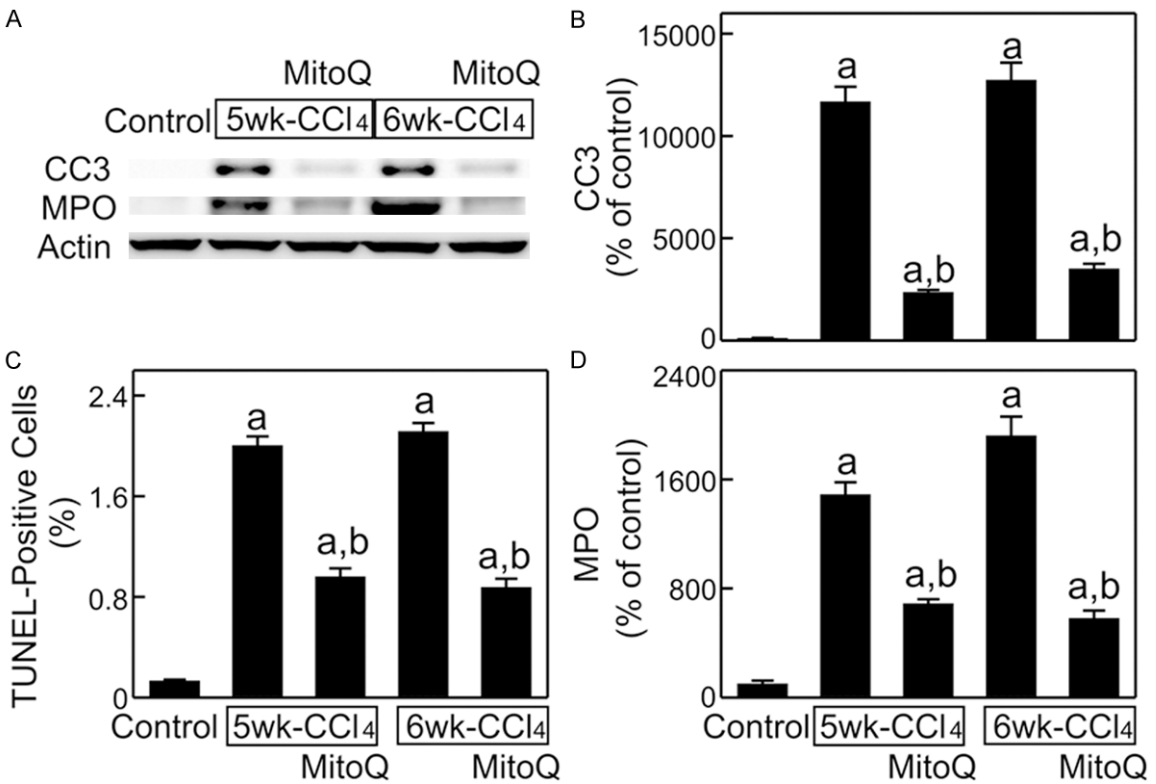

Figure 2. MitoQ inhibits apoptosis and inflammation in the liver after CCl_4 treatment in vivo. Mice were treated as in **Figure 1**, and livers were collected at 5 and 6 weeks. A: Representative immunoblot images of cleaved caspase-3 (CC3) and myeloperoxidase (MPO); B: Quantification of CC3 immunoblot images by densitometry; C: TUNEL-positive hepatocytes were counted in 10 random fields per slide as percentage of total; D: Quantification of MPO immunoblot images by densitometry. Values are means ± SEM. a, $p<0.05$ vs control; b, $p<0.05$ vs the corresponding CCl_4 group (n = 4/group).

te reader (Molecular Devices, Sunnyvale, CA). The hydroxyproline content was expressed as μg/g liver wet weight [31].

Hepatic stellate cell isolation and culture

HSCs were isolated from male Sprague-Dawley rats (500-600 g) by pronase and collagenase digestion and purified, as described [32]. Cells were cultured in standard medium (1990R with 20% serum, pH. 7.0) at 3% CO_2 and 37°C for the first 2 days and then switched to the same medium with 0.5% serum for 4 days. MitoQ (0.5-2 μM) or equal volume of vehicle (DMSO) was added to the culture medium on the second and fourth days. Morphologic features of HSCs during culture were examined by phase contrast microscopy (Nikon TE300, Nikon Co.). HSCs were harvested after 6 days of culture and lysed in the RIPA buffer. Proteins of interest in cell lysates were detected by immunoblotting as described below.

Immunoblotting

Some liver tissue was snap-frozen in liquid nitrogen during liver harvesting and kept at -80°C until use. Proteins of interest in liver tissue and HSC extracts were then detected by immunoblotting, as described previously [28]. The membranes were blotted with primary antibodies specific for cleaved caspase-3 (CC3) and actin (Cell Signaling Technology, Danvers, MA), 4-hydroxynonenal adducts (4-HNE, Alpha Diagnostic, San Antonio, TX), transforming growth factor-β1 (TGF-β1, Abcam, Cambridge, MA), collagen-I (Abcam, Cambridge, MA), Smad2/3 and phospho-Smad2/3, extracellular signal-regulated protein kinase 1/2 (ERK1/2) and phospho-ERK1/2 (Santa Cruz Biotech., Santa Cruz, CA), and myeloperoxidase (MPO), smooth muscle α-actin (α-SMA, DAKO, Carpinteria, CA) at 1:1000 to 1:3000 overnight at 4°C. Horseradish peroxidase-conjugated secondary antibodies of appropriate species were

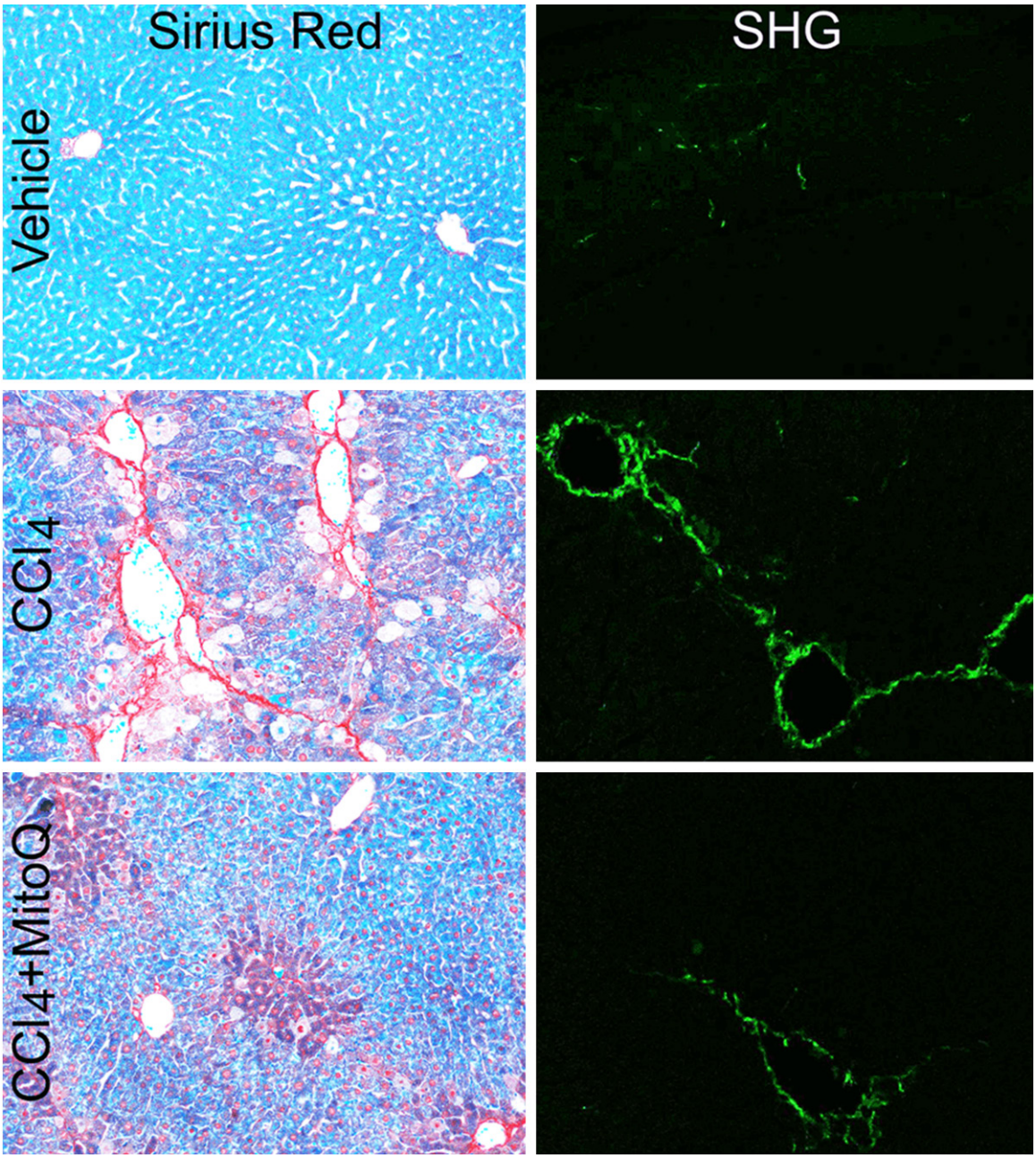

Figure 3. MitoQ inhibits liver fibrosis after CCl_4 treatment in vivo. Mice were treated as in **Figure 1**. Livers were collected at 6 weeks of CCl_4 or vehicle treatment for histology. Left: representative images of sirius red-stained liver sections. Right: representative second harmonic generation (SHG) images (n = 4/group).

applied, and detection was achieved by chemiluminescence (Pierce Biotechnology, Rockford, IL).

Detection of collagen 1α1 mRNA by quantitative real time PCR (qPCR)

Total RNA was isolated with Trizol (Invitrogen, Grand Island, NY) from liver tissue, and qPCR detection of collagen 1α1 mRNA was performed, as described elsewhere [28, 33]. The abundance of mRNAs was normalized against hypoxanthine phosphoribosyltransferase (HPRT) housekeeping gene using the ΔΔC*t* method.

Statistical analysis

Groups were compared using ANOVA plus Student-Newman-Keuls posthoc test. Data

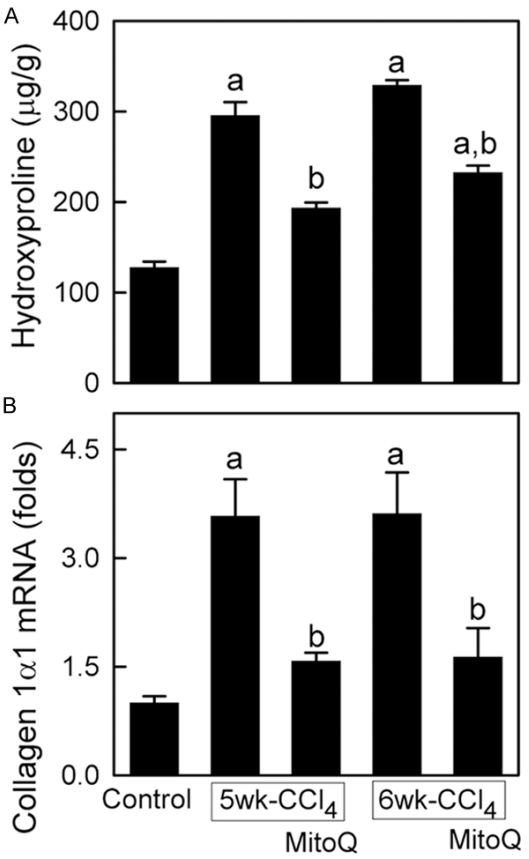

Figure 4. MitoQ decreases hydroxyproline and collagen 1α1 mRNA in the liver after CCl_4 treatment in vivo. Mice were treated as in **Figure 1**, and livers were collected at 5 and 6 weeks. A: Hydroxyproline. B: Collagen 1α1 mRNA detected by qPCR. Values are means ± SEM. a, $p<0.05$ vs control; b, $p<0.05$ vs the corresponding CCl_4 group (n = 4/group).

shown are means ± S.E.M. (4 livers per group in *in vivo* studies and 3 separate batches of HSCs per group in HSC culture studies). Differences were considered significant at $p<0.05$.

Results

MitoQ attenuates liver injury and inflammation after CCl_4 treatment in vivo

Liver injury and subsequent inflammation may contribute to development of liver fibrosis. ALT release, an indicator of liver injury, increased from ~30 U/L after vehicle treatment (corn oil and decylTPP for 6 weeks) to 410-470 U/L after 5 and 6 weeks of CCl_4 treatment (**Figure 1A**). Administration of MitoQ decreased ALT after CCl_4 to 154-182 U/L (**Figure 1A**).

No pathological changes were observed in liver tissue in the control group (corn oil and decylTPP treatment for 6 weeks, the same for all in vivo experiments) (**Figure 1B**), but cell swelling, fatty infiltration, cell death and leukocyte infiltration became overt in livers after CCl_4 treatment, primarily in the pericentral regions (**Figure 1C**). MitoQ markedly decreased these pathological changes (**Figure 1D**).

Caspase-3 mediates apoptosis. Cleaved caspase-3 (CC3) increased after 5 and 6 weeks of CCl_4 treatment (**Figure 2A** and **2B**). TUNEL-positive cells also increased, indicating apoptosis (**Figure 2C**). MitoQ markedly decreased caspase-3 activation and TUNEL staining (**Figure 2A-C**).

Myeloperoxidase (MPO), a marker of neutrophil infiltration, was essentially undetectable in the control group but increased 15-19-fold after 5 and 6 weeks of CCl_4 treatment (**Figure 2A** and **2D**). In the presence of MitoQ, MPO increased only 6-7-fold after CCl_4 treatment.

MitoQ decreases liver fibrosis after CCl_4 treatment in vivo

As expected, sirius red staining revealed fibrosis in liver sections (**Figure 3**, left panels). In the livers of control mice, sirius red stained only large portal and central structures and not the liver parenchyma (**Figure 3** and data not shown). By contrast, sirius red staining increased markedly after CCl_4 treatment, particularly in pericentral regions. MitoQ treatment substantially decreased this CCl_4-induced fibrosis (**Figure 3**, left panels). Detection of collagen by SHG imaging confirmed the marked increase of fibrosis after CCl_4, which was substantially decreased by MitoQ (**Figure 3** right panels).

Hydroxyproline, an indicator of collagen deposition, increased from 127 μg/g liver to 295 and 329 μg/g liver after 5 and 6 weeks of CCl_4 treatment, respectively (**Figure 4A**). With MitoQ treatment, hydroxyproline increased to only 193 and 232 μg/g liver after 5 and 6 weeks of CCl_4 (**Figure 4A**). Collagen 1α1 mRNA also increased ~3.6-fold after 5 and 6 weeks of CCl_4 treatment, signifying increased collagen expression (**Figure 4B**). By contrast in mice given MitoQ, collagen 1α1 mRNA only increased ~1.6-fold after CCl_4 (**Figure 4B**).

MitoQ inhibits hepatic stellate cell activation and TGF-β/Smad signaling in the liver after CCl_4 treatment in vivo

Expression of smooth muscle α-actin (α-SMA), an indicator of HSC activation, increased 4- and

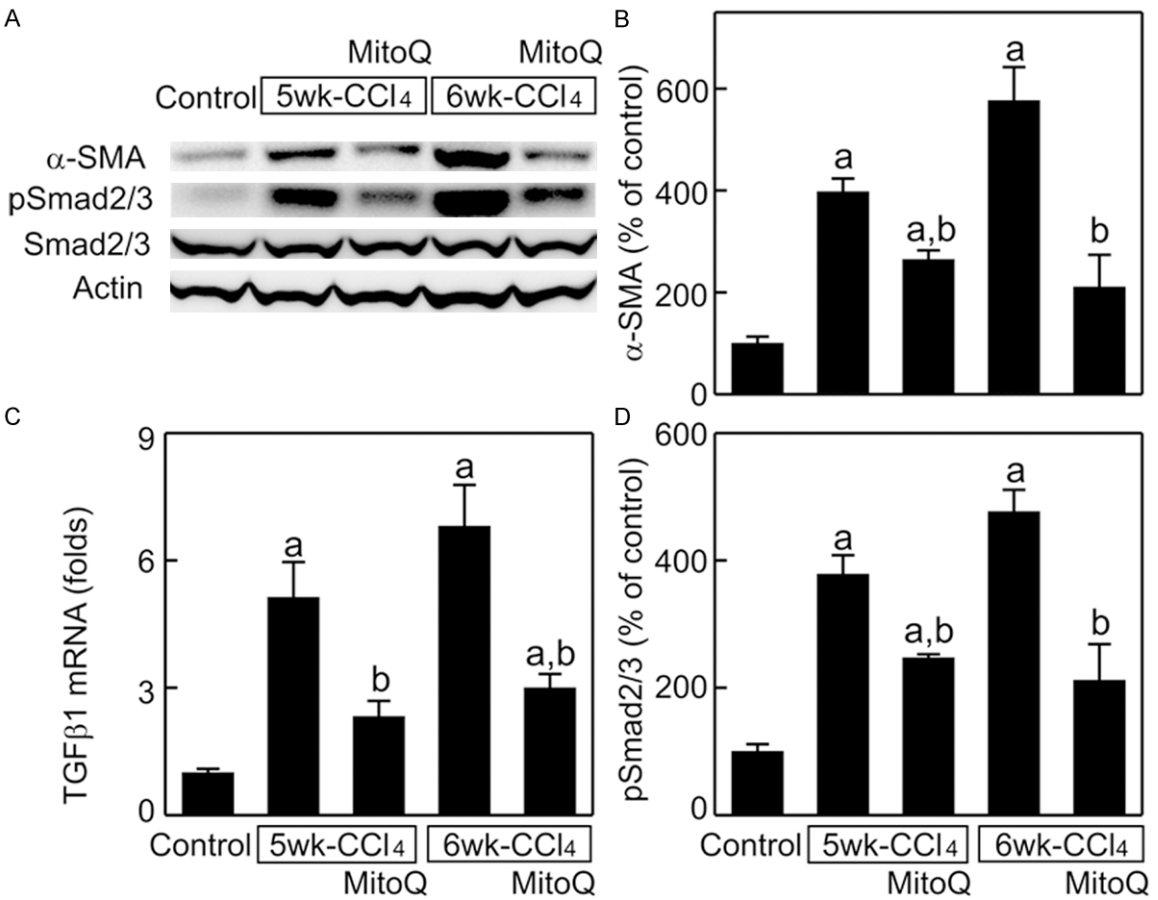

Figure 5. MitoQ inhibits stellate cell activation and TGF-β/Smad signaling in the liver after CCl_4 treatment in vivo. Mice were treated as in **Figure 1**, and livers were collected at 5 and 6 weeks. A: Representative immunoblot images of smooth muscle α-actin (α-SMA), Smad2/3, phospho-smad2/3 (pSmad2/3), and β-actin. B: Quantification of α-SMA immunoblot images by densitometry. C: Quantification of transforming growth factor-β1 (TGFβ1) mRNA by qPCR. D: Quantification of pSmad2/3 immunoblot images by densitometry. Values are means ± SEM. a, $p<0.05$ vs control; b, $p<0.05$ vs the corresponding CCl_4 group (n = 4/group).

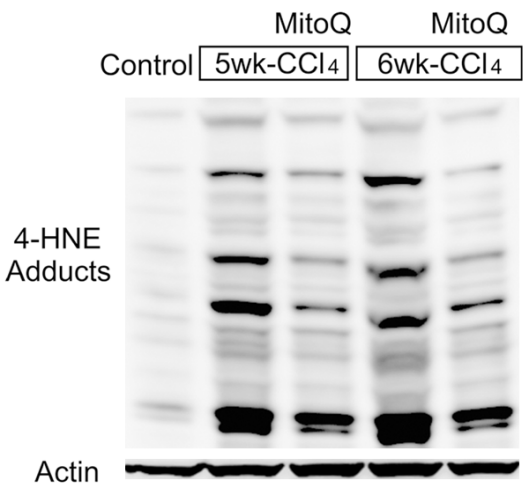

Figure 6. MitoQ inhibits oxidative stress in the liver after CCl_4 treatment in vivo. Mice were treated as in **Figure 1**, and livers were collected at 5 and 6 weeks. Shown are representative immunoblot images of 4-hydroxynonenal adducts (4-HNE) and β-actin (n = 4/group).

5.8-fold, respectively, after 5 and 6 weeks of CCl_4 treatment. MitoQ blunted these increases in α-SMA after CCl_4 (**Figure 5A** and **5B**). Profibrogenic cytokine TGF-β1 mRNA increased 5- and 6.8-fold, respectively, after 5 and 6 weeks of CCl_4 treatment in the absence of MitoQ but increased only 2.3- and 3-fold with MitoQ treatment (**Figure 5C**). Smad2/3 mediates TGF-β fibrogenic effects. Although total Smad2/3 expression was not altered after CCl_4 treatment, phospho-Smad2/3 increased 3.8- and 4.8-fold, respectively, after 5 and 6 weeks of CCl_4 treatment, indicating Smad2/3 activation. In the presence of MitoQ, phospho-Smad2/3 in-

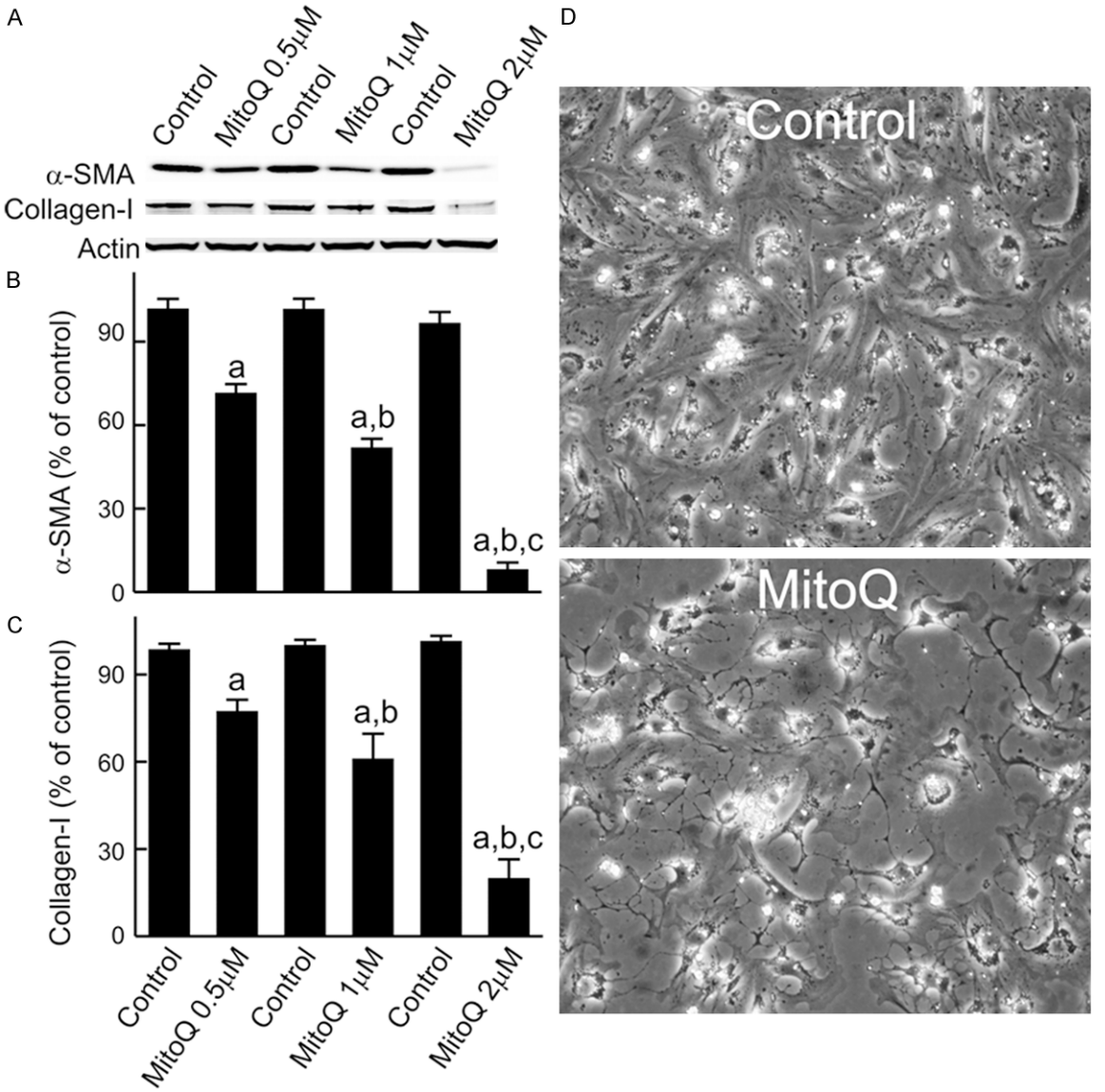

Figure 7. MitoQ inhibits stellate cell activation in vitro. HSCs were isolated from normal rats and cultured in 20% serum-containing medium. After 2 days, serum was decreased to 0.5%. MitoQ (0.5-2 μM) or an equal volume of DMSO (Control) was added at days 2 and 4, and cells were harvested at 6 days. A: Representative immunoblot images of smooth muscle α-actin (α-SMA), collagen-I, and β-actin. B: Quantification of α-SMA immunoblot images by densitometry. C. Quantification of collagen-I immunoblot images by densitometry. D: Representative images of cultured HSCs at 6 days. Values are means ± SEM. a, $p<0.05$ vs corresponding controls; b, $p<0.05$ vs 0.5 μM MitoQ. c, $p<0.05$ vs 1 μM MitoQ (n = 3/group).

creased only 2.5- and 2.1-fold, respectively (**Figure 5D**).

MitoQ decreases hepatic oxidative stress after CCl_4 treatment in vivo

4-Hydroxynonenal (4-HNE) is a product of lipid peroxidation and a widely used marker of oxidative stress. Multiple weak bands of 4-HNE adducts were observed in the livers of control mice (**Figure 6**). 4-HNE adducts increased substantially after 5 and 6 weeks of CCl_4 treatment. MitoQ blunted the production of these 4-HNE adducts (**Figure 6**).

MitoQ inhibits hepatic stellate cell activation in vitro

We next investigated the effects of MitoQ on cultured HSCs. Rat HSCs were employed, since

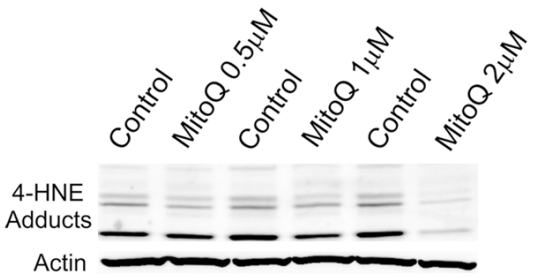

Figure 8. MitoQ decreases 4-hydroxynonenal adducts in cultured stellate cells. HSCs were isolated from normal rats and treated as described in **Figure 7**. After 6 days, cell lysates were subjected to immunoblotting to detect 4-hydroxynonenal adducts (4-HNE) and β-actin. Shown are representative immunoblot images (n = 3/group).

many more HSCs can be isolated from rat compared to mouse and because previous studies have shown that rat and mouse HSCs display very similar cell and molecular behaviors. In culture, HSCs undergo spontaneous activation, as indicated by expression of a-SMA and collagen-I (**Figure 7A-C**). With exposure to 0.5, 1 and 2 μM MitoQ, α-SMA protein expression decreased 29%, 46% and 93%, respectively, compared to controls after 6 days of culture (**Figure 7A** and **7B**). MitoQ (0.5, 1 and 2 μM) had similar effects on collagen-I protein expression, which decreased by 23%, 35% and 84%, respectively (**Figure 7A** and **7C**). Morphologically after 6 days in culture, control HSCs had a highly spread and "activated" appearance. However, HSCs exposed to MitoQ were smaller in size and rounder than control cells, consistent with suppression of HSC activation by MitoQ (**Figure 7D**).

MitoQ inhibits oxidative stress, TGF-β expression and canonical signaling in cultured hepatic stellate cells

In the lysates of control HSCs, multiple strong 4-HNE adduct bands were observed after 6 days of culture, indicating lipid peroxidation from formation of ROS (**Figure 8**). MitoQ decreased 4-HNE adduct formation in a concentration-dependent manner (**Figure 8**). Production of the profibrogenic cytokine, TGF-β1, was also reduced by 36%, 51% and 86%, respectively, by 0.5, 1 and 2 μM MitoQ compared to control cells after 6 days of culture (**Figure 9A** and **9B**). Total Smad2/3 expression was not changed by MitoQ, but phospho-Smad2/3 decreased by 21%, 41% and 87%, respectively, with 0.5, 1 and 2 μM MitoQ compared to control HSCs (**Figure 9A** and **9C**). Since ERK activation also mediates the fibrogenic effects of TGF-β, we evaluated total and phospho-ERK1/2 in 6-day cultured HSCs. Total ERK1/2 expression was not altered by MitoQ, but phospho-ERK1/2 decreased by 31%, 55% and 85%, respectively, with 0.5, 1 and 2 μM MitoQ (**Figure 9A** and **9D**).

Discussion

Despite extensive studies, effective therapies for fibrosis/cirrhosis are still lacking. Chronic liver injury leads to damage/death of hepatocytes and persistent inflammation. A complex network of profibrogenic, proinflammatory and proliferative mediators are produced during liver injury by neighboring and infiltrating cells, which leads to HSC activation and production of ECM [1, 2, 7]. No doubt, the most effective anti-fibrotic therapies are those targeting the primary stimuli of fibrogenesis, e.g., inhibition of viral hepatitis [34, 35] and iron depletion in patients with hemochromatosis [36]. Blockade of common profibrogenic and proinflammatory pathways, inhibition of HSC activation, enhancement of apoptosis, inactivation or senescence of HSCs, and/or stimulation of ECM degradation are also potential therapeutic targets.

Many previous studies have shown that ROS are important mediators of liver injury and fibrosis [8]. For example, ROS attack macromolecules (lipids, proteins, DNA), inhibit mitochondrial function, damage cell membranes, and induce necrosis and apoptosis, which may subsequently lead to initiation of fibrogenesis [9, 10, 37]. ROS also amplify the inflammatory response. Damage of hepatocytes by ROS causes release of inflammasomes and other damage-associated molecular pattern molecules (DAMPs, e.g. HMGB1), which are potent inflammatory mediators [38, 39]. ROS cause nuclear factor-κB activation that subsequently leads to formation of proinflammary cytokines/chemokines (e.g., TNFα, interleukin-1, macrophage inflammatory protein 1&2, CXC chemokine-10) and adhesion molecules which attract leukocytes [40, 41]. Infiltrating leukocytes are activated to produce more ROS, causing a vicious cycle.

ROS also stimulate the production/activation of profibrotic and proliferative mediators (e.g.,

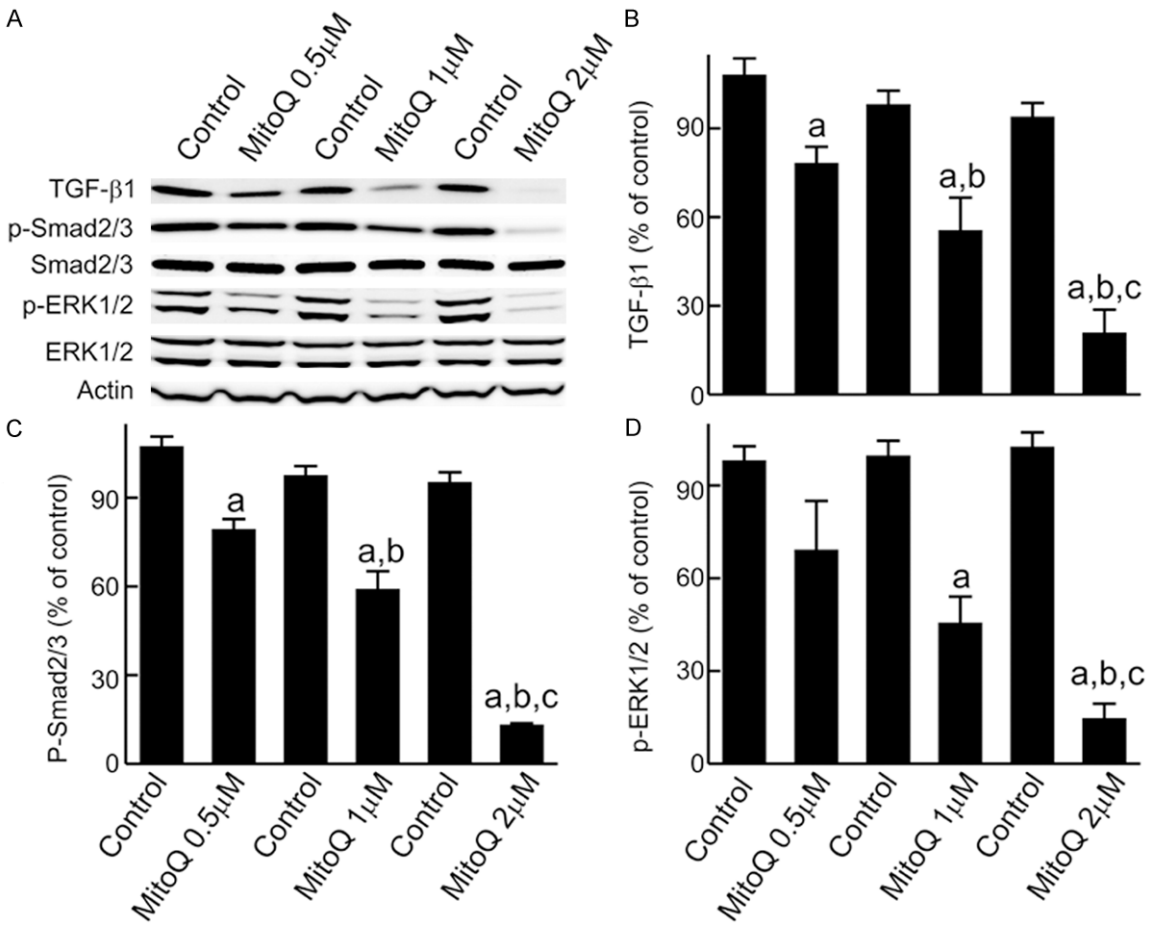

Figure 9. MitoQ inhibits TGF-β, Smad and ERK signaling in cultured stellate cells. HSCs were isolated from normal rats and cultured as described in **Figure 7**. After 6 days, cell lysates were collected to detect transforming growth factor-β1 (TGF-β1), Smad2/3, phospho-Smad2/3 (p-Smad2/3), extracellular signal-regulated protein kinase 1/2 (ERK1/2), phospho-ERK1/2 (p-ERK1/2) and β-actin. A: Representative immunoblot images. B: Quantification of TGF-β1 immunoblot images by densitometry. C: Quantification of p-Smad2/3 immunoblot images by densitometry. D: Quantification of p-ERK1/2 immunoblot images by densitometry. Values are means ± SEM. a, $p<0.05$ vs corresponding controls; b, $p<0.05$ vs 0.5 μM MitoQ. c, $p<0.05$ vs 1 μM MitoQ (n = 3/group).

TGF-β, connective tissue growth factor, platelet-derived growth factor) in Kupffer cells, cholangiocytes, endothelial cells, and infiltrating platelets and inflammatory cells [8, 11, 12, 43, 42]. Moreover, oxidative stress directly activates HSCs [44, 45]. Antioxidants inhibit upregulation of tissue metallopeptidase inhibitor 1 after bile duct ligation, a molecule that inhibits metalloproteinases which are responsible for ECM degradation [46]. Since ROS play important roles in many aspects of pathogenesis of liver fibrosis, inhibiting ROS formation or accelerating their degradation are promising therapeutic targets for prevention or treatment of fibrosis. Indeed, vitamin E has been shown to prevent progression of fibrosis in non-alcoholic steatohepatitis patients [30].

While there are many different sources of ROS formation in cells, such as NADPH oxidase, xanthine oxidase, cytochrome P450 and peroxisomes, mitochondria are recognized as a major source of ROS in numerous pathophysiological settings. During mitochondrial respiration, some electrons escape the electron transport chain prematurely to form superoxide at Complexes I and III [47]. Production of ROS from mitochondria increases markedly in many pathological conditions, including CCl_4 intoxication [47, 48]. Mitochondria are also a target of ROS, resulting in induction of the mitochondrial permeability transition, mitochondrial membrane potential collapse, failure of oxidative phosphorylation, and oncotic cell death [49]. Mitochondrial swelling causes release of pro-apoptot-

ic factors such as cytochrome *c*, leading to apoptosis [49], and apoptotic bodies from hepatocytes can cause HSC activation [50].

Previous studies also show that compared to nuclear DNA, mitochondrial DNA is more sensitive to oxidative damage due to the lack of histone protection and the proximity to the major sites of ROS production [51]. Emerging evidence shows that mitochondrial dysfunction leads to inflammatory reactions by increasing the formation and activation of the inflammatory signaling platform NLRP3-inflammasomes [52, 53]. Mitochondrial damage causes release of mitochondrial DNA, which is known to induce inflammation [13, 54, 55]. Mitochondrial oxidative stress increases formation/activation of profibrogenic TGF-β [56, 57]. Mitochondrial uncoupling, increased consumption of oxygen, and subsequent liver hypoxia can induce hypoxia inducible factor-1α [58]. Inflammation, TGF-β and hypoxia inducible factor-1α all promote liver fibrosis [59-61]. Together, mitochondrial damage/dysfunction may be a critical step in liver injury, inflammation and fibrosis.

Previously, we showed that overexpression of mitochondrial SOD protected against cholestatic liver injury and fibrosis to a much greater extent than overexpression of cytosolic SOD, suggesting a mitochondrial targeted antioxidant may have greater benefit compared to untargeted antioxidants [15]. In this study, we explored the effects of MitoQ, a mitochondria-targeted antioxidant [19], on liver fibrosis in vivo. We demonstrated that MitoQ treatment in vivo decreased oxidative stress (4-HNE), inhibited formation of the profibrogenic cytokine TGF-β, blocked downstream signaling pathways of TGF-β (Smad activation) and suppressed liver fibrosis (sirius red staining, SHG, hydroxyproline, collagen synthesis) after exposure to CCl_4. Moreover, MitoQ also decreased hepatocellular injury/death (ALT, necrosis, apoptosis) and reduced subsequent inflammation (MPO), which may contribute to the attenuation of liver fibrosis by MitoQ. HSC activation is an essential step in liver fibrosis. MitoQ not only inhibited HSC activation *in vivo* but also suppressed spontaneous HSC activation in culture. Therefore in addition to protecting against hepatocellular injury and thus inhibiting subsequent inflammatory and fibrogenic responses, MitoQ also decreased liver fibrosis by direct inhibition of HSC activation.

Together, this study demonstrates that mitochondrial oxidative stress plays an essential role in liver fibrosis after CCl_4 and demonstrates that the mitochondria-targeted antioxidant MitoQ is an effective therapeutic strategy against liver fibrosis. Moreover, MitoQ is orally active and can be safely administered over the long-term [62]. Therefore, MitoQ is suitable for clinical application and may be a promising drug for prevention and/or treatment of liver fibrosis in humans.

Acknowledgements

This study was supported, in part, by Grants from the National Institute of Health [DK70844, DK037034] and the Chinese National Natural Foundation [Grant 81470878]. The Cell & Molecular Imaging Core of the Hollings Cancer Center at the Medical University of South Carolina supported by NIH Grant 1P30 CA138313 provided instrumentation and assistance for SHG microscopy. Animals were housed in the Animal Resources at Medical University of South Carolina supported by NIH Grant C06 RR015455.

Address correspondence to: Dr. Zhi Zhong, Departments of Drug Discovery & Biomedical Sciences, Medical University of South Carolina, Charleston, SC 29425, USA. E-mail: zhong@musc.edu

References

[1] Friedman SL. Liver fibrosis -- from bench to bedside. J Hepatol 2003; 38 Suppl 1: S38-S53.

[2] Berardis S, Dwisthi SP, Najimi M, Sokal EM. Use of mesenchymal stem cells to treat liver fibrosis: Current situation and future prospects. World J Gastroenterol 2015; 21: 742-758.

[3] Schuppan D and Kim YO. Evolving therapies for liver fibrosis. J Clin Invest 2013; 123: 1887-1901.

[4] Wertheim JA, Petrowsky H, Saab S, Kupiec-Weglinski JW, Busuttil RW. Major Challenges Limiting Liver Transplantation in the United States. Am J Transplant 2011; 11: 1773-1784.

[5] Kisseleva T and Brenner DA. Role of hepatic stellate cells in fibrogenesis and the reversal of fibrosis. J Gastroenterol Hepatol 2007; 22 Suppl 1: S73-S78.

[6] Rockey DC. Hepatic fibrosis, stellate cells, and portal hypertension. Clin Liver Dis 2006; 10: 459-79, vii-viii.

[7] Guo CJ, Pan Q, Cheng T, Jiang B, Chen GY, Li DG. Changes in microRNAs associated with he-

patic stellate cell activation status identify signaling pathways. FEBS J 2009; 276: 5163-5176.
[8] Sanchez-Valle V, Chavez-Tapia NC, Uribe M, Mendez-Sanchez N. Role of oxidative stress and molecular changes in liver fibrosis: a review. Curr Med Chem 2012; 19: 4850-4860.
[9] Parola M and Robino G. Oxidative stress-related molecules and liver fibrosis. J Hepatol 2001; 35: 297-306.
[10] Robino G, Zamara E, Novo E, Dianzani MU, Parola M. 4-Hydroxy-2,3-alkenals as signal molecules modulating proliferative and adaptative cell responses. Biofactors 2001; 15: 103-106.
[11] Jaeschke H. Reactive oxygen and mechanisms of inflammatory liver injury. J Gastroenterol Hepatol 2000; 15: 718-724.
[12] Ha HL, Shin HJ, Feitelson MA, Yu DY. Oxidative stress and antioxidants in hepatic pathogenesis. World J Gastroenterol 2010; 16: 6035-6043.
[13] Brenner C, Galluzzi L, Kepp O, Kroemer G. Decoding cell death signals in liver inflammation. J Hepatol 2013; 59: 583-594.
[14] Zhong Z, Froh M, Lehnert M, Schoonhoven R, Yang L, Lind H, Lemasters JJ, Thurman RG. Polyphenols from Camellia sinenesis attenuate experimental cholestasis-induced liver fibrosis in rats. Am J Physiol Gastrointest Liver Physiol 2003; 285: G1004-G1013.
[15] Zhong Z, Froh M, Wheeler MD, Smutney O, Lehmann TG, Thurman RG. Viral gene delivery of superoxide dismutase attenuates experimental cholestasis-induced liver fibrosis in the rat. Gene Ther 2002; 9: 183-191.
[16] Lemasters JJ, Theruvath TP, Zhong Z, Nieminen AL. Mitochondrial calcium and the permeability transition in cell death. Biochim Biophys Acta 2009; 1787: 1395-1401.
[17] Birch-Machin MA and Turnbull DM. Assaying mitochondrial respiratory complex activity in mitochondria isolated from human cells and tissues. Methods Cell Biol 2001; 65: 97-117.
[18] Oyewole AO and Birch-Machin MA. Mitochondrial-targeted antioxidants. FASEB J 2015; 28: 485-94.
[19] James AM, Cocheme HM, Smith RA, Murphy MP. Interactions of mitochondria-targeted and untargeted ubiquinones with the mitochondrial respiratory chain and reactive oxygen species. Implications for the use of exogenous ubiquinones as therapies and experimental tools. J Biol Chem 2005; 280: 21295-21312.
[20] Adlam VJ, Harrison JC, Porteous CM, James AM, Smith RA, Murphy MP, Sammut IA. Targeting an antioxidant to mitochondria decreases cardiac ischemia-reperfusion injury. FASEB J 2005; 19: 1088-1095.
[21] James AM, Cocheme HM, Murphy MP. Mitochondria-targeted redox probes as tools in the study of oxidative damage and ageing. Mech Ageing Dev 2005; 126: 982-986.
[22] Dashdorj A, Jyothi KR, Lim S, Jo A, Nguyen MN, Ha J, Yoon KS, Kim HJ, Park JH, Murphy MP, Kim SS. Mitochondria-targeted antioxidant MitoQ ameliorates experimental mouse colitis by suppressing NLRP3 inflammasome-mediated inflammatory cytokines. BMC Med 2013; 11: 178.
[23] Supinski GS, Murphy MP, Callahan LA. MitoQ administration prevents endotoxin-induced cardiac dysfunction. Am J Physiol Regul Integr Comp Physiol 2009; 297: R1095-R1102.
[24] Gane EJ, Weilert F, Orr DW, Keogh GF, Gibson M, Lockhart MM, Frampton CM, Taylor KM, Smith RA, Murphy MP. The mitochondria-targeted anti-oxidant mitoquinone decreases liver damage in a phase II study of hepatitis C patients. Liver Int 2010; 30: 1019-1026.
[25] Snow BJ, Rolfe FL, Lockhart MM, Frampton CM, O'Sullivan JD, Fung V, Smith RA, Murphy MP, Taylor KM. A double-blind, placebo-controlled study to assess the mitochondria-targeted antioxidant MitoQ as a disease-modifying therapy in Parkinson's disease. Mov Disord 2010; 25: 1670-1674.
[26] Aoyama T, Inokuchi S, Brenner DA, Seki E. CX3CL1-CX3CR1 interaction prevents carbon tetrachloride-induced liver inflammation and fibrosis in mice. Hepatology 2010; 52: 1390-1400.
[27] Troeger JS, Mederacke I, Gwak GY, Dapito DH, Mu X, Hsu CC, Pradere JP, Friedman RA, Schwabe RF. Deactivation of hepatic stellate cells during liver fibrosis resolution in mice. Gastroenterology 2012; 143: 1073-1083.
[28] Rehman H, Ramshesh VK, Theruvath TP, Kim I, Currin RT, Giri S, Lemasters JJ, Zhong Z. NIM811, a Mitochondrial Permeability Transition Inhibitor, Attenuates Cholestatic Liver Injury But Not Fibrosis in Mice. J Pharmacol Exp Ther 2008; 327: 699-706.
[29] Zhong Z, Theruvath TP, Currin RT, Waldmeier PC, Lemasters JJ. NIM811, a Mitochondrial Permeability Transition Inhibitor, Prevents Mitochondrial Depolarization in Small-for-Size Rat Liver Grafts. Am J Transplant 2007; 7: 1103-1111.
[30] Campagnola PJ and Loew LM. Second-harmonic imaging microscopy for visualizing biomolecular arrays in cells, tissues and organisms. Nat Biotechnol 2003; 21: 1356-1360.
[31] Reddy GK and Enwemeka CS. A simplified method for the analysis of hydroxyproline in biological tissues. Clin Biochem 1996; 29: 225-229.
[32] Shi Z and Rockey DC. Interferon-gamma-mediated inhibition of serum response factor-dependent smooth muscle-specific gene expression. J Biol Chem 2010; 285: 32415-32424.

[33] Liu Q, Rehman H, Krishnasamy Y, Haque K, Schnellmann RG, Lemasters JJ, Zhong Z. Amphiregulin Stimulates Liver Regeneration After Small-for-Size Mouse Liver Transplantation. Am J Transplant 2012; 12: 2052-61.

[34] Poynard T, McHutchison J, Manns M, Trepo C, Lindsay K, Goodman Z, Ling MH, Albrecht J. Impact of pegylated interferon alfa-2b and ribavirin on liver fibrosis in patients with chronic hepatitis C. Gastroenterology 2002; 122: 1303-1313.

[35] Hadziyannis SJ, Tassopoulos NC, Heathcote EJ, Chang TT, Kitis G, Rizzetto M, Marcellin P, Lim SG, Goodman Z, Wulfsohn MS, Xiong S, Fry J, Brosgart CL. Adefovir dipivoxil for the treatment of hepatitis B antigen-negative chronic hepatitis B. N Engl J Med 2003; 348: 800-807.

[36] Powell LW and Kerr JF. Reversal of "cirrhosis" in idiopathic haemochromatosis following long-term intensive venesection therapy. Australas Ann Med 1970; 19: 54-57.

[37] Singh R and Czaja MJ. Regulation of hepatocyte apoptosis by oxidative stress. J Gastroenterol Hepatol 2007; 22 Suppl 1: S45-S48.

[38] Chen R, Hou W, Zhang Q, Kang R, Fan XG, Tang D. Emerging role of high-mobility group box 1 (HMGB1) in liver diseases. Mol Med 2013; 19: 357-366.

[39] Gauley J and Pisetsky DS. The translocation of HMGB1 during cell activation and cell death. Autoimmunity 2009; 42: 299-301.

[40] Jaeschke H, Ho YS, Fisher MA, Lawson JA, Farhood A. Glutathione peroxidase-deficient mice are more susceptible to neutrophil-mediated hepatic parenchymal cell injury during endotoxemia: importance of an intracellular oxidant stress. Hepatology 1999; 29: 443-450.

[41] Czaja MJ. Cell signaling in oxidative stress-induced liver injury. Semin Liver Dis 2007; 27: 378-389.

[42] Sies H and Cadenas E. Oxidative stress: damage to intact cells and organs. Philos Trans R Soc Lond B Biol Sci 1985; 311: 617-631.

[43] Bilzer M, Roggel F, Gerbes AL. Role of Kupffer cells in host defense and liver disease. Liver Int 2006; 26: 1175-1186.

[44] Galli A, Svegliati-Baroni G, Ceni E, Milani S, Ridolfi F, Salzano R, Tarocchi M, Grappone C, Pellegrini G, Benedetti A, Surrenti C, Casini A. Oxidative stress stimulates proliferation and invasiveness of hepatic stellate cells via a MMP2-mediated mechanism. Hepatology 2005; 41: 1074-1084.

[45] Friedman SL. Mechanisms of hepatic fibrogenesis. Gastroenterology 2008; 134: 1655-1669.

[46] Shen K, Feng X, Su R, Xie H, Zhou L, Zheng S. Epigallocatechin 3-gallate ameliorates bile duct ligation induced liver injury in mice by modulation of mitochondrial oxidative stress and inflammation. PLoS One 2015; 10: e0126278

[47] Kovacic P, Pozos RS, Somanathan R, Shangari N, O'Brien PJ. Mechanism of mitochondrial uncouplers, inhibitors, and toxins: focus on electron transfer, free radicals, and structure-activity relationships. Curr Med Chem 2005; 12: 2601-2623.

[48] Sudheesh NP, Ajith TA, Mathew J, Nima N, Janardhanan KK. Ganoderma lucidum protects liver mitochondrial oxidative stress and improves the activity of electron transport chain in carbon tetrachloride intoxicated rats. Hepatol Res 2012; 42: 181-191.

[49] Kim JS, He L, Lemasters JJ. Mitochondrial permeability transition: a common pathway to necrosis and apoptosis. Biochem Biophys Res Commun 2003; 304: 463-470.

[50] Lee TF, Lin YL, Huang YT. Kaerophyllin inhibits hepatic stellate cell activation by apoptotic bodies from hepatocytes. Liver Int 2011; 31: 618-629.

[51] Akhmedov AT and Marin-Garcia J. Mitochondrial DNA maintenance: an appraisal. Mol Cell Biochem 2015; 409: 283-305.

[52] Gurung P, Lukens JR, Kanneganti TD. Mitochondria: diversity in the regulation of the NLRP3 inflammasome. Trends Mol Med 2014; 21: 193-201.

[53] Cherry AD and Piantadosi CA. Regulation of mitochondrial biogenesis and its intersection with inflammatory responses. Antioxid Redox Signal 2015; 22: 965-76.

[54] Mathew A, Lindsley TA, Sheridan A, Bhoiwala DL, Hushmendy SF, Yager EJ, Ruggiero EA, Crawford DR. Degraded mitochondrial DNA is a newly identified subtype of the damage associated molecular pattern (DAMP) family and possible trigger of neurodegeneration. J Alzheimers Dis 2012; 30: 617-627.

[55] Pinti M, Cevenini E, Nasi M, De BS, Salvioli S, Monti D, Benatti S, Gibellini L, Cotichini R, Stazi MA, Trenti T, Franceschi C, Cossarizza A. Circulating mitochondrial DNA increases with age and is a familiar trait: Implications for "inflamm-aging". Eur J Immunol 2014; 44: 1552-1562.

[56] Barnard JA, Lyons RM, Moses HL. The cell biology of transforming growth factor beta. Biochim Biophys Acta 1990; 1032: 79-87.

[57] Yue J and Mulder KM. Transforming growth factor-beta signal transduction in epithelial cells. Pharmacol Ther 2001; 91: 1-34.

[58] Zhong Z, Ramshesh VK, Rehman H, Liu Q, Theruvath TP, Krishnasamy Y, Lemasters JJ. Acute ethanol causes hepatic mitochondrial depolarization in mice: role of ethanol metabolism. PLoS One 2014; 9: e91308.

[59] Gressner AM and Weiskirchen R. Modern pathogenetic concepts of liver fibrosis suggest stellate cells and TGF-beta as major players and therapeutic targets. J Cell Mol Med 2006; 10: 76-99.

[60] Wang Y, Huang Y, Guan F, Xiao Y, Deng J, Chen H, Chen X, Li J, Huang H, Shi C. Hypoxia-inducible factor-1alpha and MAPK co-regulate activation of hepatic stellate cells upon hypoxia stimulation. PLoS One 2013; 8: e74051.

[61] Troeger JS and Schwabe RF. Hypoxia and hypoxia-inducible factor 1alpha: potential links between angiogenesis and fibrogenesis in hepatic stellate cells. Liver Int 2011; 31: 143-145.

[62] Rodriguez-Cuenca S, Cocheme HM, Logan A, Abakumova I, Prime TA, Rose C, Vidal-Puig A, Smith AC, Rubinsztein DC, Fearnley IM, Jones BA, Pope S, Heales SJ, Lam BY, Neogi SG, McFarlane I, James AM, Smith RA, Murphy MP. Consequences of long-term oral administration of the mitochondria-targeted antioxidant MitoQ to wild-type mice. Free Radic Biol Med 2010; 48: 161-172.